A molecular loaded dice

Aidibi, Youssef; Beaujean, Pierre; Quertinmont, Jean; Stiennon, Julien; Hodée, Maxime; Leriche, Philippe; Berthet, Jérôme; Delbaere, Stéphanie; Champagne, Benoît; Sanguinet, Lionel

Published in:
Dyes and pigments

DOI:
10.1016/j.dyepig.2022.110270

Publication date:
2022

Document Version
Publisher's PDF, also known as Version of record

Dyes and Pigments 202 (2022) 110270

Contents lists available at ScienceDirect

Dyes and Pigments

journal homepage: www.elsevier.com/locate/dyepig

A molecular loaded dice: When the π conjugation breaks the statistical addressability of an octastate multimodal molecular switch

Youssef Aidibi [a,1], Pierre Beaujean [b,1], Jean Quertinmont [b], Julien Stiennon [b], Maxime Hodée [b], Philippe Leriche [a], Jérôme Berthet [c], Stéphanie Delbaere [c,**], Benoît Champagne [b,***], Lionel Sanguinet [a,*]

[a] MOLTECH, Anjou UMR CNRS 6200, Groupe Systèmes conjugués linéaires, University of Angers, 2 boulevard Lavoisier, 49045, Angers, France
[b] Theoretical Chemistry Laboratory, Unit of Theoretical and Structural Physical Chemistry, Namur Institute of Structured Matter, University of Namur, B-5000, Namur, Belgium
[c] Univ Lille, INSERM, CHU Lille, UMR-S 1172, Lille Neuroscience and Cognition Research Center, 59000, Lille, France

ARTICLE INFO

Keywords:
Molecular switch
Indolino-oxazolidine
Electrochromism
Halochromism

ABSTRACT

The elaboration of multichromophoric system which can undergo a reversible transformation over more than two different states can be easily performed by the covalent assembly of several identical switching subunits around a central node. However, the selective addressability of each of them still represents a challenging task. This study reports on the elaboration of multichromophoric systems incorporating three identical indolino-oxazolidine (BOX) moieties as multimodal addressable units. Depending of the open/closed oxazolidine ring status of each of them, these systems can be interconverted between four different states in stepwise manner by using indifferently acid addition or electrochemical stimulation. More important, we have demonstrated by using a dissymmetric triarylamine node that the classical statistical BOX opening is broken then reaching a regioselective addressability. The switching of the three identical BOX units differentiated by their π conjugated junction to the central core follows a preferential order leading to the preponderant and successive formation of only four forms over the eight theoretically and equally expected. To provide limitations and outlooks for such strategy, their switching capacities have been rationalized by DFT calculations.

1. Introduction

Due to their numerous application fields, the elaboration of molecular switches continues to raise a large attention. Indeed, these molecular systems are able to undergo a reversible conversion between at least 2 metastable states under the application of an external stimulation which allows for inducing a modulation of their molecular physicochemical properties [1]. During the last decades, the number of stimuli able to undergo these changes has increased and include pH changes [2], light irradiation [3], electrochemical potential [4], temperature [4,5], and pressure [6,7] to name the most common. Among those, one may imagine numerous applications for such systems on optical data storage, molecular logic gate, medical imaging, magnetism, and molecular motors to name a few [8–10].

If a simple molecular switch allows under stimulation to control a 0/1 signal, a more complex system presenting several switches, controlled by one or several stimuli may allow much more complex combinations of responses, and potentially a storage/sensing capacity heavily improved [11–13]. Following this approach, numerous multichromophoric systems combining different switches have been developed especially photo- and redox-active materials due to their promising applications in data storage materials or molecular logic gates [14–16]. However, the selective addressability of the different constitutive switching units is still challenging when several identical photochromic [17,18] or electrochromic units [19] are combined. As example, numerous studies dedicated on multichromophoric systems involving several diarylethene (DAE) units, one of the most famous photochromes [20–31], have revealed either a lack of photoreactivity [32] or random

** Corresponding author.
*** Corresponding author.
* Corresponding author.
E-mail addresses: stephanie.delbaere@univ-lille.fr (S. Delbaere), benoit.champagne@unamur.be (B. Champagne), lionel.sanguinet@univ-angers.fr (L. Sanguinet).
[1] **Y. Aidibi** and **P. Beaujean** contributed equally to this work.

https://doi.org/10.1016/j.dyepig.2022.110270
Received 5 December 2021; Received in revised form 21 March 2022; Accepted 21 March 2022
Available online 5 April 2022

switching behavior depending on the nature of the core used to combine them. Consecutively, many efforts continue to be devoted to optimize the substitution pattern of such multichromophoric systems in order to combine photoactivity, selective addressability and molecular properties modulation [33,34].

Another approach consists to develop multi-stimuli-responsiveness molecular systems where each switchable unit can be addressed individually by using orthogonal stimuli [35]. In this framework, indolino [2,1-b]oxazolidine derivatives (later referenced as BOX) have particularly caught our attention. Firstly reported at the end of the last century [36], they exhibit several assets: (*i*) two metastable states, generally referenced as Open (O) and Closed (C) in respect to the oxazolidine ring status, exhibiting strong differences of optical and electronic properties, (*ii*) an easy preparation in few steps from cheap and commercially available compounds, (*iii*) a large panel of available functionalizations in positions 2 and 5, and finally [37,38], (*iv*) some multimodal switching abilities as light irradiation or pH changes can be used indifferently to induce the conversion from colorless C to colorful O state [39,40]. An UV light induces effectively the C–O bond cleavage leading to the oxazolidine ring opening and corresponding zwitterionic form but this later is spontaneously converted in the presence of water traces to its open protonated form. More recently, their multimodal switching abilities were extended to electrochemical stimulation. This conversion from closed to open protonated form results from the direct BOX unit oxidation [41] or involves an indirect electromediated process when a redox active system is present on position 2 [42]. In both cases, the oxidation of the colorless form conducts to the formation of the corresponding radical cation mainly localized either on the indoline moiety or on the adjacent pi conjugated system in position 2. Unstable by nature, this this latter is involved in a spontaneous chemical rearrangement leading to the opening of the oxazolidine ring and the generation of an alkoxy radical, which is able to abstract an Hydrogen atom to surrounding media and conducts to observe at the end the generation of the protonated open form [37,42,43]. The benefits to this uncommon switchable unit for the elaboration of performant multichromophoric systems have been already reported. As example, the functionalization of a DAE unit by one or two BOX has led to multiresponsive molecular systems exhibiting up to 8 and 13 different metastable states respectively [43,44]. Beside their combination with other switchable units, pure BOX multichromophoric systems have been also envisioned. Nowadays, limited to very simple π conjugated linear systems bearing two BOX terminations, these materials allow a step by step pH-, optical and redox-switching of the two units leading to a logic 0, 1, 2 system with contrasted, linear and, more importantly, nonlinear optical properties [38,45,46].

As a new step in the direction of more complex logic systems, we present here our efforts to graft three BOX units in the periphery of a triarylamine node. By analogy to previous reported systems, it expects to lead to multichromophoric systems exhibiting at least 4 discrete states when symmetrical cores are used (Schemes 1). More important, by using dissymetrically substituted amine bearing three different π conjugated systems, we expect to overcome the highly challenging task of regioselectivite addressability of BOX units. Based on a modulation of the electronic interactions with the central redox center, we aim the BOX opening in a preferential order leading to observe a step by step switching of the system between only 4 over the 8 potential different forms of this system (Scheme 1).

For such reason, some unsymmetrical triBOX systems have been elaborated by grafting three BOX units on the periphery of a redox active triarylamine bearing a phenyl (Ph); a phenylthiophene (ThPh) and a biphenyl (PhPh) as π-conjugated linkers (Scheme 2). Their regioselective addressability and switching capacities have been explored by spectroscopy and electrochemistry and compared to the performances of their symmetrical analogs (Scheme 2). Moreover, their behavior has been rationalized by the help of density functional theory (DFT) calculations to provide limitations and outlooks for such strategy.

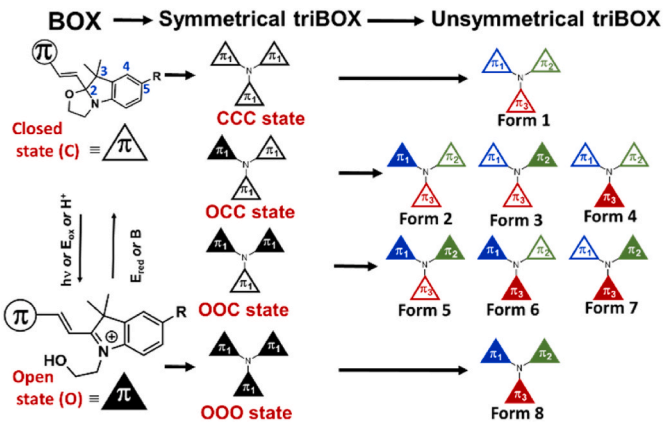

Scheme 1. Schematic representation of the 4 different states and associated forms of a triBOX derivative as function of the open (O) or closed (C) status of the three BOX units.

2. Results and discussion

2.1. Synthesis

The triphenylamine constitutes the basic node of an important group of modern electroactive functional materials especially for organic, dye-sensitized and perovskite solar cells applications [47]. Its functionalization is well-documented and many works report on their formylation, bromination and palladium catalyzed coupling. All three are largely involved in the modification of the π-conjugated system which is known to induce a strong modification of the molecular electronic properties. For this study, we have prepared different triarylamine derivatives where each terminal BOX unit is connected to the central nitrogen atom by three different π-conjugated linkers: a simple phenyl, a phenylthiophene and a biphenyl. As consequence, each of the three BOX units will exhibit a direct electronic coupling to the aromatic amine core acting as a strong electron-donating group. Knowing that the BOX switching properties are generally affected by the nature of the substituents in positions 5 and 2, we plan to take advantage of this variation of electronic coupling to drive the opening of the three BOX in a predefine sequential order. To obtain our desired symmetrical and dissymmetrical multi-BOX systems, we have followed a convergent strategy. It consists on one hand, to prepare corresponding triarylamine derivatives bearing three carboxaldehyde terminal functions and, on the other hand, some indolino[2,1-b]oxazolidines bearing different substituents. During previous studies, the introduction of a fluorine atom and a methyl group in position 5 has already facilitated the identification of the metastable states and the electrochemical process respectively (*vide infra*) [41,45].

Concerning the substituted indolino[2,1-b]oxazolidines, their synthesis has been already reported and does not represent particular difficulties. When non-commercially available, the substituted trimethylindolenines are obtained by Fisher indole synthesis from the corresponding hydrazine. Their quaternarization by 2-iodoethanol following by a base treatment allows the formation of the oxazolidine ring and the formation of the desired compounds in good yield (65–76%). The dissymmetrical aryl amine preparation is only slightly more fastidious than symmetrical ones as the scaffold is constructed step by step. It starts by the insertion of bromine atoms in each para position of the 4-(diphenylamino)benzaldehyde by NBS at 0 °C in THF. By performing two Suzuki-coupling reactions with successively (i) (5-formylthiophen-2-yl)boronic acid, and then (4-formylphenyl)boronic acid, the desired dissymmetrical triarylamine is obtained in only three steps with an overall yield of 46% (Scheme 3).

The covalent assembly of the BOX units on the central triarylamine core results from a simple condensation between both components. If

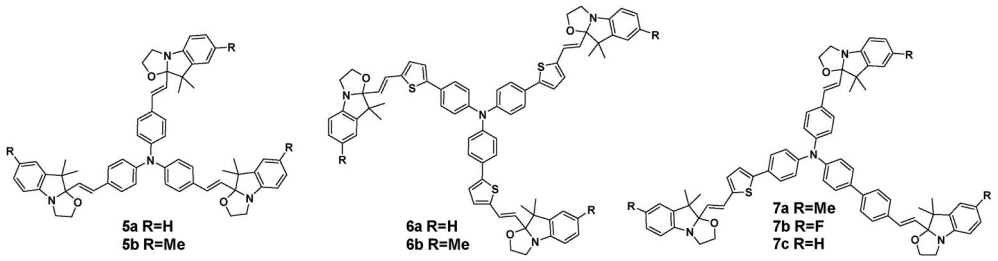

Scheme 2. Structure of the 4 symmetrical (**5a-b, 6a-b)** and 3 unsymmetrical (**7a-c**) triBOX derivatives under their **CCC** state.

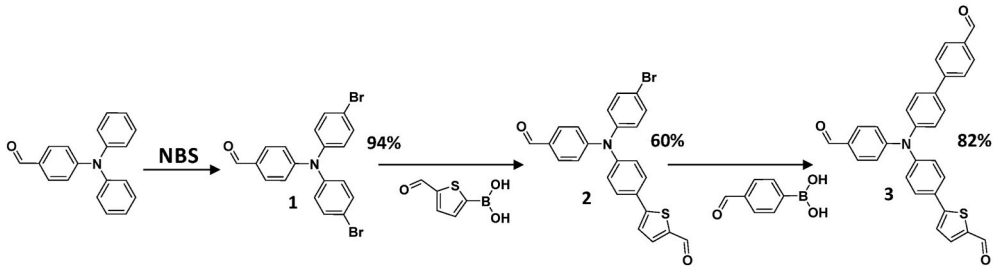

Scheme 3. Synthesis of the tricarboxaldehyde amine involving 3 different linkers: a phenyl (Ph), a phenylthiophene (PhTh) and a biphenyl (PhPh).

many experimental conditions can be applied to perform such reaction [37,38,48], we have used here a silica-mediated procedure known to improve the reactivity of the trimethylindolino[2,1-b]oxazolidine derivatives [38]. After heating during 7 h at 100 °C, these solvent-free conditions allow the formation of the different targeted systems with moderate to good yields (44–77%) depending on the purification difficulties (Scheme 4).

2.2. Acidochromic properties of triBOX

When all BOX units remain under their closed status, all compounds exhibit low absorption properties in the visible range. In fact, the spectra of compounds **5**–**7** have similar shape and reveal one simple absorption band with a maximum absorption wavelength in the near UV domain (Fig. 1).

As expected, the extension of the π-conjugated system induces a bathochromic shift. This is particularly true for symmetrical compounds where the addition of a thiophene unit on each arm in **6** is associated with a 42 nm shift relative to triarylamine derivatives **5**. At the opposite, the dissymetrization of the triarylamine core induces only a moderate variation of the maximum absorption wavelength (17 nm shift). Under their fully closed states, the variation of the substituent in position 5 of the indoline does not induce a modification of the optical properties whatever the nature of the central core (Table 1). Such behavior can be explained by the breaking of the conjugation between the triarylamine moiety and the indoline due to the sp^3 hybridization of the carbons in position 2 [49]. As expected, the addition of some acid on the fully closed form leads instantaneously to a drastic modification of the UV–visible spectra. In all cases, we notice the appearance of an intense broad band in the visible 455–655 nm range as well as a concomitant decrease of the band in the near visible range. Based on our previous studies on BOX derivatives, this expected coloration translates

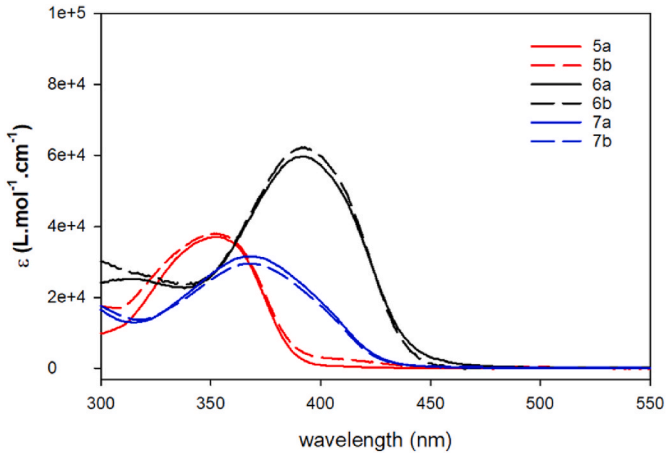

Fig. 1. UV visible spectra of compounds **5–7** under their fully closed states, CCC, and evolution of their maximum absorption wavelength (λ_{max} in nm) under acid stimulation as function of the open (O) or closed (C) status of the three BOX units.

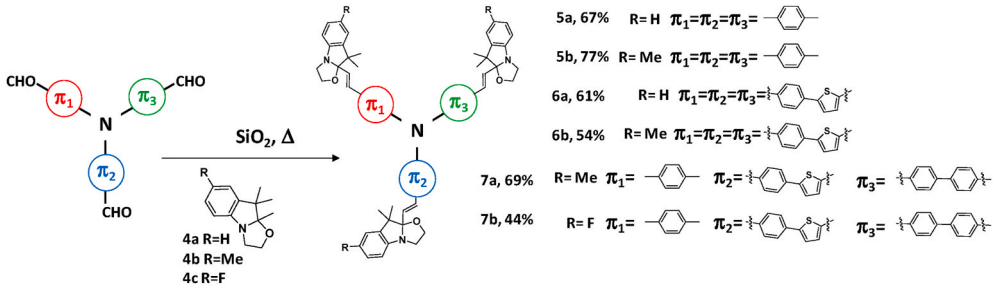

Scheme 4. Synthesis of the 4 symmetrical and 2 unsymmetrical triBOX derivatives by silica mediated procedure from the corresponding tris-carboxaldehyde amine.

Table 1
Main transition details of the different forms and simulated UV/vis absorption spectra of **7c** as a function of the level of opening according their relative proportions.

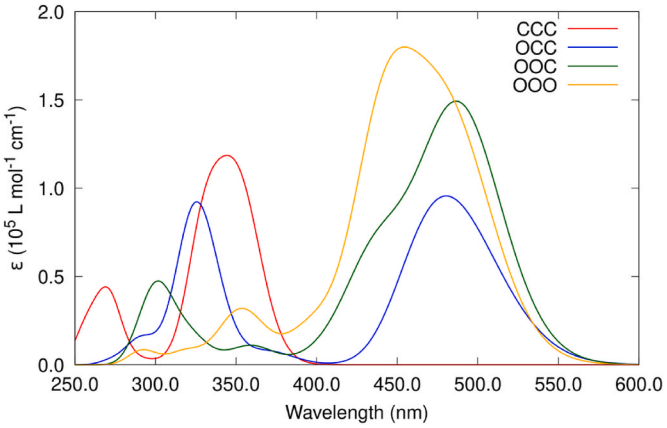

State	Form	%	λ_{ge}	ΔE_{ge}	f_{ge}	λ_{max}	ΔE_{max}
CCC	1	100	353	3.51	1.44	344	3.60
OCC	2	61	473	2.62	1.83	480	2.58
	3	37	501	2.47	1.66		
	4	2	454	2.73	1.45		
OOC	5	87	490	2.53	2.34	486	2.55
	6	11	475	2.61	1.95		
	7	2	495	2.50	2.06		
OOO	8	100	486	2.55	1.93	454	2.73

Vertical excitation wavelengths (λ_{ge}, nm), vertical excitation energies (ΔE_{ge}, eV) and oscillator strengths (f_{ge}) of the first excited state. The maximal excitation wavelengths (λ_{max}, nm) and energy (ΔE_{max}, eV) of the different states, accounting for their relative proportions, are also reported. The averages are weighted using the populations of conformers at 298.15 K as calculated at the ωB97X-D/6-311-G(d)/IEF-PCM (ACN) level of theory.

unambiguously the opening of the oxazolidine rings under acidic stimulation leading to the establishment of a charge transfer band between the electron donor triarylamine moiety and the generated indoleninium acting as an electron withdrawing group. Interestingly, an irregular evolution of the UV–visible spectra along the titration with acid aliquots is noticed for all systems suggesting a stepwise BOX opening under stimulation [45,46]. As example, the titration of symmetrical compounds is presented on Fig. 2. Up to one equivalent, the strong decrease of the band intensity at 351(392) nm, assigned to the **CCC** form of **5b (6b)**, is concomitant with the appearance of an unique band centered at 551(572) nm. Exhibiting one isosbestic point at 376(427) nm, it testifies an equilibrium between two species. Due to the symmetrical nature of the system, it translates the selective opening of only one BOX among the three units, and as a consequence the conversion

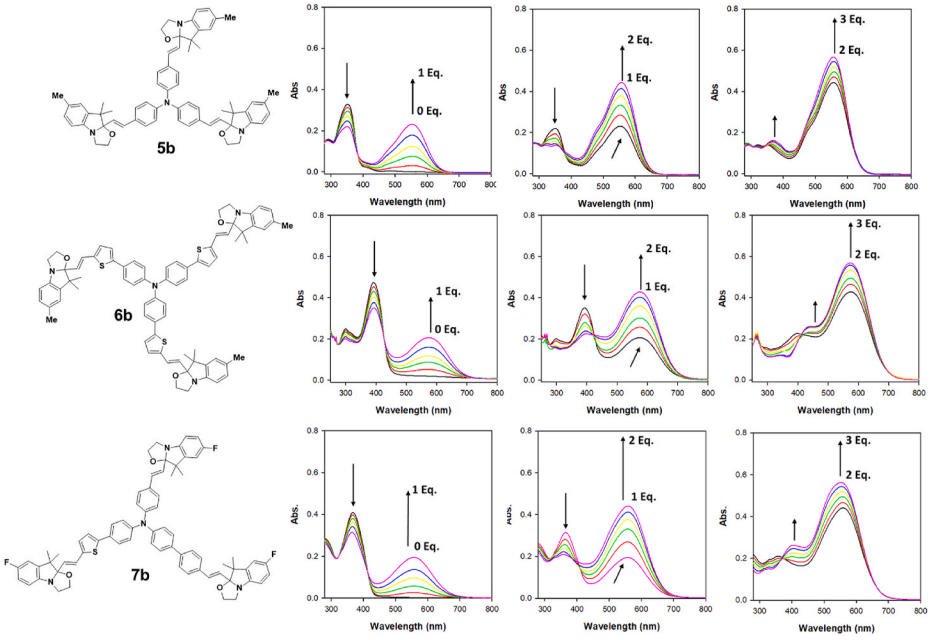

Fig. 2. Variation of the UV–visible spectrum of **5b** (9 10^{-6}M), **6b** (7 10^{-6}M) and **7b** (9 10^{-6}M) in ACN upon the addition of HCl aliquots from 0 to 1.0 eq. (left), from 1.0 to 2.0 eq (middle) and from 2.0 to 3.0 eq (right).

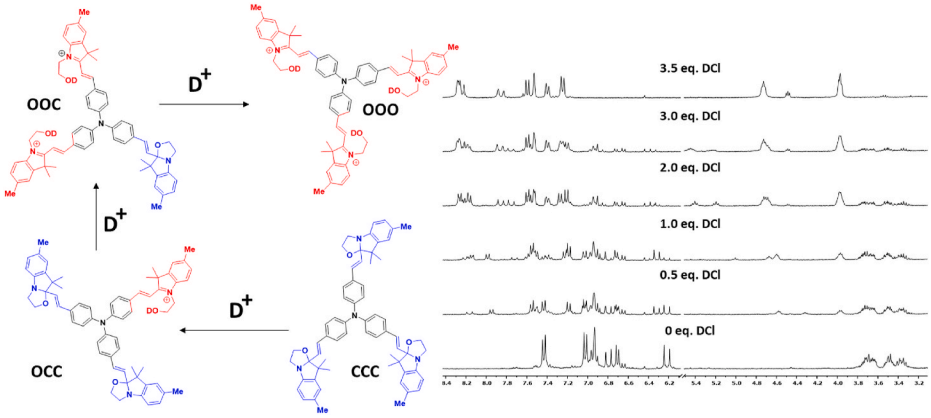

Fig. 3. Variation of the ^{1}H NMR spectra of compound **5b** (4.62 mM) in ACN solution upon the addition of DCl aliquots at 20 °C translating the successive formation of **OCC**, **OOC** and **OOO** states.

from **CCC** to **OCC** state. The addition of acid up to two equivalents induces first the reduction of the band at 351(392) nm and, second a slight bathochromic shift from 551(572) nm to 559(574) nm as well as a hyperchromic effect of the main absorption band. The previous isosbestic point is not conserved and a new one is noticed at 382(420) nm suggesting a second equilibrium. This later can be reasonably assigned to the second selective BOX opening and the system conversion from **OCC** to **OOC** state. Surprisingly, increasing the quantity of acid up to 3 equivalents leads to observe mainly a hyperchromic effect on the main visible absorption band with almost no change in the absorption maximum wavelength. In addition, the appearance of a new higher energy band at 364(428) nm is noticed. Once again, the previous isosbestic point is replaced by a new one at 345(407) nm translating the presence of a third equilibrium assigned to the selective transformation of the system from **OOC** to **OOO** state.

To confirm this stepwise switching upon the addition of acid and identify unambiguously the formation of the different states, the same titration was monitored by ^{1}H NMR spectroscopy. As example, the titration performed on compound **5b** is presented on Fig. 3. Under its initial state **CCC**, the compound **5b** exhibits simple spectra with typical spectral signature of closed BOX systems such as a series of multiplets for the methylene groups adjacent to the nitrogen and oxygen atoms (5 and 6) ranging from 3.4 to 3.9 ppm and three singlets at 2.33, 1.46 and 1.19 ppm for each methyl groups of the indolino-oxazolidine unit. Additionally, we notice only one doublet at 6.22 ppm assigned to one ethylenic proton. Exhibiting a vicinal coupling constant around 16Hz, it allows us to confirm only the presence of the full *trans* isomer as well as its perfect symmetrical nature. As very distinguishable signal of **CCC** state, it can be used to follow the switching behavior of BOX derivatives under various stimulations [44]. As soon as the addition of acid starts, its intensity decreases and an important complexification of the spectrum is noticed. Especially, two deshielded doublets (J ~ 16 Hz) appear (6.3 and 8.4 ppm). Based on our previous investigation [43,45,46,50], we can assign the most shielded to an ethylenic proton attached to a closed BOX. The opening BOX induces a much stronger low field shift of them. For this reason, the second doublet is assigned to an ethylenic proton attached to an open BOX. Below 1 eq of acid, both signals exhibit an integration ratio close to 2 which translates the selective opening of only one BOX, generating the **OCC** state. The spectrum complexification increases when the addition of acid is pursued up to two equivalents. Indeed, the two previous doublets (6.3, 8.4 ppm) disappear and are replaced by a new set of peaks. Especially, a new doublet with a 16Hz vicinal coupling constant is detected at 6.4 ppm. The low field shift of this signal corresponding to an ethylenic bond attached to a closed BOX is in agreement with the opening of a second BOX unit and the generation of the **OOC** state. Finally, a simplification of the spectrum is noticed after the addition of 3.5 equivalents. A new set of two doublets (J~16Hz) is detected at 7.9 and 8.3 ppm translating the opening of the remaining third BOX unit and the generation of the **OOO** state exhibiting a C_{3v} symmetry with fully *trans* configuration of the ethylenic junctions.

No drastic changes in the acidochromic response are observed between unsymmetrical triBOX and their symmetrical analogs. Similarly, to compounds **5** and **6**, an irregular evolution of the UV–visible spectra along the titration with acid aliquots is also noticed with compounds **7a** (not presented here) and **7b** (Fig. 2) suggesting a stepwise switching of the system. As mentioned above (Scheme 1), the **OCC** state resulting from the stimulation of compounds **7** under their **CCC** state should lead to a statistical mixture of the three different forms **2**, **3** and **4**. As for the symmetrical analogs, different isosbestic points are noticed upon the addition of acid. As shown for **7b** on Fig. 2, the isosbestic points at 412 and 323 nm observed at the beginning of titration (0–1 eq.) are successively substituted by others, at 406 (1–2eq) and 367 nm (2–3 eq.) along the titration with HCl. This behavior suggests a successive equilibrium between two species, and then suggests that the acid stimulation of the system leads to a regioselective addressability with the opening of the 3 different BOX units in a specific order. As UV–visible spectroscopy did not allow us to extract sufficient structural information, NMR spectroscopy was used to unambiguously confirm the regioselective addressability of the unsymmetrical systems. Under their closed form, both compounds **7a** and **7b** exhibit complex ^{1}H NMR spectrum. However, typical closed BOX signature can be observed such as four successive multiplets ranging from 3.9 to 3.4 ppm characterizing the oxazolidine rings as well as the presence in aliphatic region of intense peaks at *ca.* 1.2 and 1.4 ppm corresponding to the geminal methyl groups of the BOX moieties. In addition, **7a** and **7b** present three well-separated doublets with a J coupling constant of 16 Hz for the three vinylic protons. By 2D NMR experiments and comparison with symmetrical analogs, it was possible to assign each of these signals to each different arm constituting the unsymmetrical compounds. As example for **7a**, (Figures S4- S6). the doublets at 6.12, 6.27 and 6.39 ppm are assigned to the vinylic protons connecting a closed BOX unit to the thiophene-phenyl, the phenyl, and the biphenyl systems, respectively. The signals of the vinylic protons are very helpful to monitor the switching of systems involving several BOX units [46]. We observe effectively the concomitant generation of new doublets at low field (ranging from 8.2 to 8.5 ppm) and the generation of new signals around 4.0 and 4.5 ppm translating the formation of a pendant ethyloxy chain, thus confirming the opening of the BOX unit under acidic stimulation. Ranging from 6.0 to 6.5 ppm, a multiplication of signals corresponding to the vinylic protons is observed upon the addition of DCl aliquots. They can be separated in three distinct groups, each of them being associated to one type of linker (δ PhPh > δ Ph > δ ThPh) bearing a closed BOX. An excess of acid leads to the complete disappearance of signals in 6.0–6.5 ppm range and of the multiplets below 4.0 ppm, evidencing the

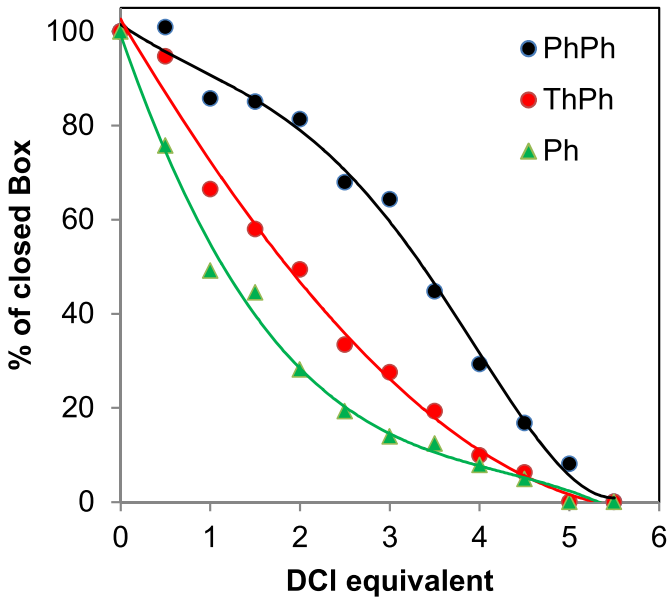

Fig. 4. Variation of the ^{1}H NMR spectra of compound **5b** (4.62 mM) in ACN solution upon the addition of DCl aliquots at 20 °C translating the successive formation of **OCC**, **OOC** and **OOO** states.

complete conversion of the system into the **OOO** state (form **8**, Figs. S7 and S11). Due to signal overlap, it was not possible to perform the integration of each form separately, but we could follow the decrease of the peak-intensities of the closed BOX unit for each of the three different linkers (Fig. 4). The global evolution of the 3 groups of signals at δ 6.35–6.45 (PhPh), δ 6.22–6.32 (Ph) and δ 6.08–6.18 (ThPh) reveals a non-statistical repartition upon the amount of acid added. The BOX units are addressed firstly when borne by Ph, secondly by ThPh and thirdly by PhPh.

To clarify the regioselective addressability according to the π-system nature, the fluorine nucleus in **7b** was used as NMR probe. Signals between −124.5 and −125 ppm characterize fluorine in closed BOX unit while signals between −111 and −114 ppm evidence fluorine in open BOX unit (Fig. S12). The initial **CCC** state of **7b** presents three peaks at −124.90, −124.87 and −124.76 ppm. First additions of acid led to the appearance of signals at −111.7, −112.67 ppm and −113.00 ppm, each being characteristic of the three forms **2**, **3**, **4** with one open BOX unit. They are associated with two new signals in the range −124 to −125 ppm corresponding to the two other BOX units remaining under their closed status. This confirms the generation of the **OCC** state into three forms (**2**, **3** and **4**, see Scheme S1). By continuing the acid addition, the **OOC** state under its three forms is observed (two signals between −111 and −114 ppm and one signal between −124.5 and −125 ppm are observed three times, for **5**, **6** and **7**). Finally, an excess of acid produces the last state **OOO** (form **8**). with its three signals at −111.42, −112.32 and −112.6 ppm The solubility of this last state is poor leading to some partial precipitation as already observed with other multi-BOX derivatives [45]. The ^{19}F NMR resolution being better, the evolution of the peak-intensities could be measured for the eight forms (Fig. 5). In agreement with the response of **7a**, a non-statistical distribution between forms **2**, **3** and **4** is observed in the **OCC** state translating a regioselective addressability. As demonstrated by the integration of the different signals, the formation of the **OCC** state results mainly from the opening of the BOX unit attached to the phenyl arm (form **2**), while the opening of the BOX on the biphenyl group (form **4**) is the less promoted. This preferential opening order is kept for the **OOC** state of the second unit which follows the same trends. The form **5** is predominantly accumulated, as it has the open BOX attached to phenyl and phenyl-thienyl groups, when the forms **6** and **7** are as expected less generated because they require the opening of the BOX attached to the biphenyl group.

To rationalize this behavior, DFT and TD-DFT calculations were performed on symmetrical and unsymmetrical systems **6a** and **7c** without any substituent on position 5 as they did not change the switching sequence and they have a tiny impact on the optical properties (*vide infra*). In both cases, the main experimental evolutions of the optical properties upon the addition of acid are well reproduced.

Concerning the symmetrical compound **6a**, we observe (i) the substantial bathochromic shift with the first BOX opening (140 nm theoretical shift vs 180 nm experimental shift) (ii) the strong hyperchromic effect on the main visible absorption band induced by the subsequent BOX opening (the predicted ε of the **OOO** state should theoretically present an epsilon three times higher than for **OCC,** explained by degeneresecence**,** when a factor 2.7 is experimentally noticed), and finally (iii) the negligible shifts of the maximal absorption wavelength induced by the second and third BOX openings. While BOX units are generally considered as independent under their closed form, the stepwise conversion of the system can be largely explained by the help of theoretical calculations. In fact, we observe that the Gibbs free energy, ΔG^0 decreases with the successive protonation reactions. As example for compound **6a** with trifluoroacetic acid (TFA), ΔG^0 drops from −20.4 kJ/mol for the first BOX opening to −16.1 and −13.7 kJ/mol for the second and third protonations, respectively. The opening of a BOX leads to the generation of an indoleninium moiety, which acts as a strong electron withdrawing group. As consequence, this raising difficulty to open subsequent BOX units can be simply explained by a decrease of the electron donor character of the central π-core that is involved in the stabilization of the corresponding cationic form. As carried out with **6a**, we have determined the ΔG^0 for the first, second and third BOX opening of **7c**, following each possible chemical process (Scheme 5) when TFA is used as acid.

First, we observe that ΔG^0 increases with the successive protonation reactions whatever the chemical process corroborating the stepwise conversion of the system. More important, the BOX units borne by the Ph and ThPh linkers are preferentially addressed due to the lowest ΔG^0 (-28.7 and −27.3 kJ/mol respectively) in agreement with our experimental observations as only traces of O(PhPh)C(Ph)C(ThPh) (form **4**) were detected when **7b** is treated with one equivalent of HCl. On the

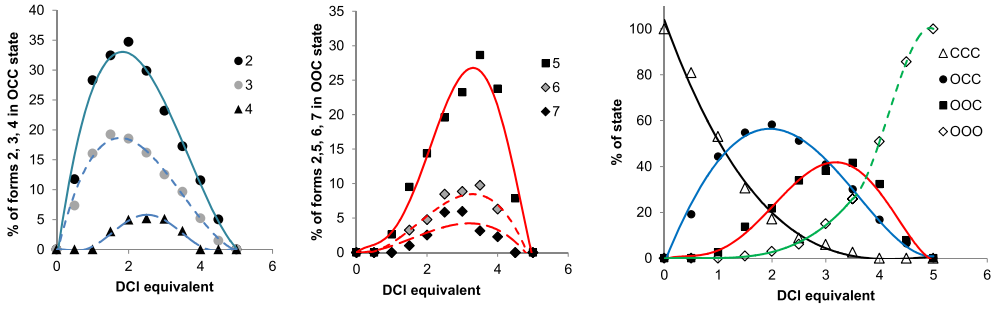

Fig. 5. Quantification of the forms in OCC and OOC states and of the 4 different states of compound **7b** (1 mM) in ACN upon addition of DCl aliquots.

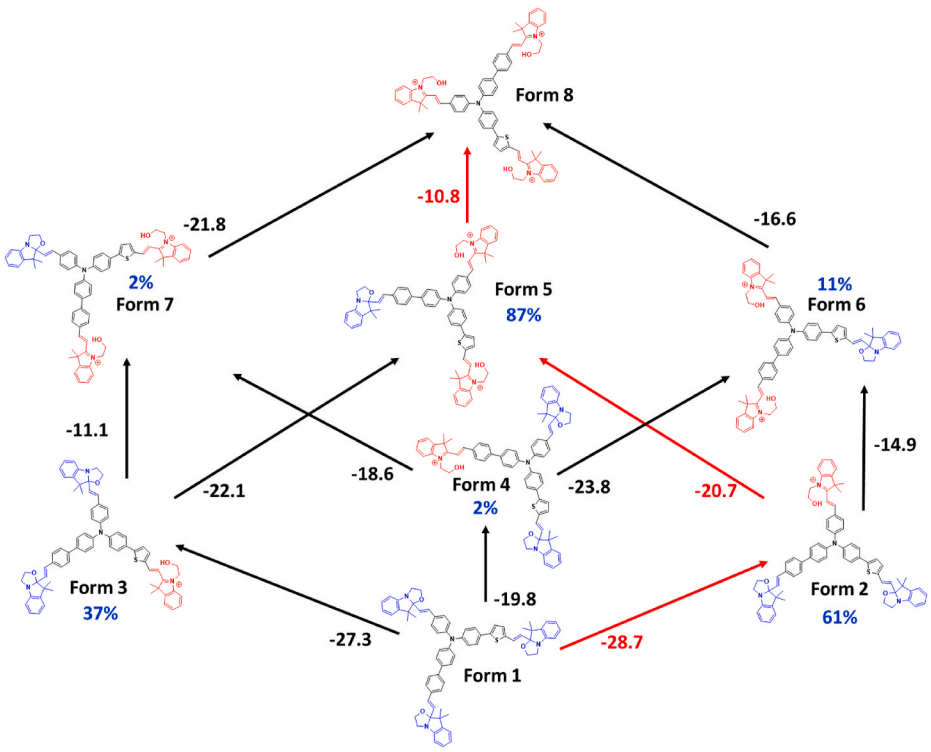

Scheme 5. Free Gibbs energy (ΔG^0, kJ/mol) of the successive protonation reactions of **7c** as a function of the level of opening (**CCC**, **OCC**, **OOC** and **OOO**) as calculated at the ωB97X-D/6-311-G(d)/IEF-PCM (ACN) level of theory. The arrows indicate the change of free enthalpy of the 3 successive protonations and the red arrows indicate the most spontaneous sequence of openings.

other hand, this small difference of ΔG^0 between both chemical processes explains certainly why a perfect regioselective addressability is not reached but it is sufficient to obtain the preponderant formation of form **2** (**Ph(O)ThPh(C)PhPh(C)**, ~61%) over form **3** (**Ph(C)ThPh(O)PhPh(C)**, ~37%). The unfavorable opening of the BOX borne by the biphenyl is also noticed during the second protonation process. Once again, it can be supported by the evolution of the Gibbs free energy of corresponding reactions. The differences of ΔG^0 between the three chemical processes leading to each form of the **OOC** state are similar to those observed for the **OCC** state (~10 kJ/mol). We can then assume that this behavior is not only driven by the variation of the electron donor character of the system but also by the difference of π-conjugation of the linker bearing the BOX unit. To tweak the simulation of the acidochromic behavior of **7c**, we have considered the different conformers of each form that exhibit a non-negligible weight within the Maxwell-Boltzmann statistics. On this basis, the relative proportions of the different forms have been estimated for each state and reported in Table 1. As we can see, theoretical calculations reproduce the experimental observations. As example, we notice the preponderant formation of form **2** (61%) over form **3** (37%) by a factor 1.68 in well agreement with the 1.85 ratio experimentally measured for compound **7b**.

To rationalize the variation of the optical properties of compounds **7** upon the addition of acid aliquots, the relative proportion of the different forms of the systems have to be considered. Indeed, the optical properties of the system are affected by the nature of the linker bearing the open BOX unit(s). This is illustrated in Table 1 where, for the **OCC** state of **7c**, opening the BOX on the PhPh, Ph, and PhTh π-linker results in bathochromic shifts of 101, 120, and 148 nm, respectively. Similarly, for the **OOC** state the λ_{max} values differ by 20 nm depending on which BOX is open or closed (Table 1). Taking in account the difference of optical properties between the different forms constituting the **OCC** and **OOC** states as well as their relative proportions, the global variation of optical properties of **7c** upon the addition of acid aliquots have been simulated (Table 1). The first BOX opening conducts to an impressive bathochromic shift of the maximum absorption wavelength (from 344 to 480 nm). The subtle variation of the maximal absorption wavelength (from 480 to 486 nm) and the hyperchromic effect (ε is enhanced by a factor 1.5) induces by switching from **OCC** to **OOC** are also in well

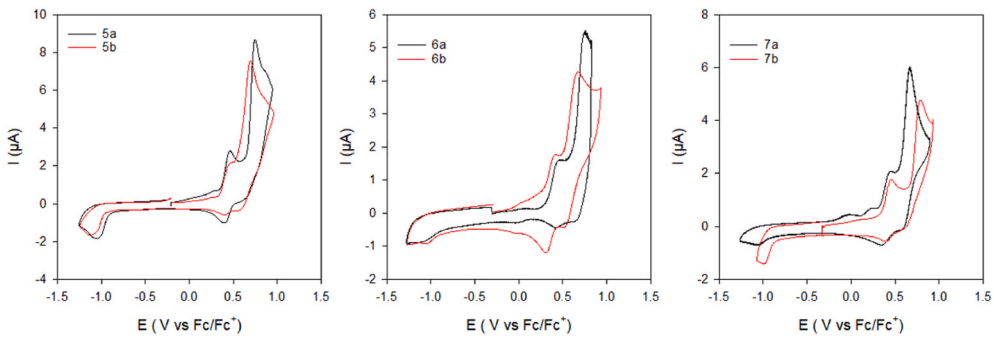

Fig. 6. Cyclic voltammetry of the different triBOX derivatives in ACN with $TBAPF_6$ as electrolyte (0.1 M) on Pt working electrode at 100 mV s^{-1}.

agreement with the experimental observations. They can be explained by a slight improvement of the averaged values of vertical excitation wavelengths and higher averaged oscillator strengths between the **OCC** and **OOC** states. Finally, TD-DFT calculations reproduce well the hyperchromic effect but overestimate the bathochromic shift induced by the last BOX opening, with 486 and 454 nm as maximum absorption wavelengths for the **OOC** and **OOO** states, respectively.

2.3. Electrochromic properties of triBOX

As mentioned above, an electrochemical stimulation can also lead to the opening of the BOX units either by their direct oxidation or by an electromediated process when they are associated to an electroactive moiety. In this context, the electrochemical behaviors of the different molecular systems have been investigated by Cyclic Voltammetry (CV) in ACN. As shown in Fig. 6, all compounds exhibit similar behavior with two successive oxidation processes at 0.4–0.5 and 0.65–0.78V. Quasi-irreversible at lower scan rate, the first one is largely affected by the nature of the π-system borne by the central nitrogen atom. Compounds **5b** and **6b** exhibit the highest (0.47 V) and the lowest (0.41 V) oxidation potential, respectively, whereas the unsymmetrical compound **7b** present an intermediate value (0.45 V). This signal is assigned to the oxidation of the central π-conjugated core leading to the generation of the corresponding radical cation and supported by studies on triarylamine electrochemical behavior [51]. The radical cation of triphenylamine is known to be stable except when no substituent is present in para positions where it could undergo a dimerization process leading to tetraphenylbenzidine [52,53]. As consequence, the pseudo irreversibility of this signal seems to indicate that the radical cation is delocalized until the close vicinity of a BOX unit inducing its opening, as already observed with other redox active systems [42,45,54]. Concerning **6b**, the extension of the π-conjugated system by adding 3 thiophene units conducts to improve the radical cation stability. At 100 mV/s, a quasi-reversible signal is observed whereas **5b** exhibits an almost irreversible peak in similar conditions (Fig. S15). Nevertheless, the reversibility in **6b** is reduced when the scan rate is decreased to 20 mV/s indicating that the electro-induced BOX opening due to an electromediated process requires longer time in this case.

The second oxidation process is more affected by the nature of the substituent in position 5 of the BOX than by the nature of the π-conjugated core itself. Compounds **5b**, **6b** and **7a** with a methyl group in position 5 present very close anodic peak potentials at 0.69, 0.66 and 0.66V. At the opposite, changing the methyl group by a fluorine atom conducts to observe an anodic shift of 0.12 V from **7a** to **7b**. Based on our previous studies on electrochemical behavior of BOX [41], we can then assign this second oxidation process to the oxidation of the remaining closed BOX unit. Indeed, under their closed forms, the BOX units behave independently to each other due to their sp^3 carbon in position 2. This direct oxidation induces also their opening as evidenced by the irreversibility of the signal and the appearance of a signal at negative potential range (~−1.0 V) on the back scan but certainly without noticeable selectivity as oxidation of all of them happens at very close potential.

To put in evidence an electromediated process leading to the stepwise switching of these systems, the titration with a chemical oxidant monitored by UV–visible spectroscopy is certainly the most convenient technique. In fact, spectro-electrochemistry measurements can present here some drawbacks. Generally, they are not able to distinguish between the stepwise switching of multiBOX systems, and the generation of long-lived radical cation exhibiting some visible absorption bands can complicate the interpretation of the UV–visible spectrum modifications [45,54]. To perform such titration, $NOSbF_6$ exhibiting an oxidation potential of 0.87 V is generally used as oxidizing agent [55]. As expected, the oxidant addition to the different systems under their **CCC** state induces a drastic change of the UV–visible spectra. More important, it leads to identical spectra as those obtained after stimulation with an excess of acid and the initial spectrum can be recovered after treatment with an excess of base such as triethylamine demonstrating the multimodal switching ability of these systems. As example, Fig. 7 shows the results obtained with **7b** in more details. The addition of the first equivalent of $NOSbF_6$ leads to the appearance of a unique band centered at 558 nm assigned to the opening of one BOX moiety per molecule and the generation of a mixture of forms **2, 3** and **4** (*vide infra*) associated with the concomitant decrease of the form **1** characteristic band at 368 nm. As observed with acid, by increasing the quantity of oxidant up to two equivalents, the low energy band intensity with a tiny bathochromic shift (559 nm) is increased and new isosbestic points are established. It translates the generation of forms **5**, **6** and **7** corresponding to the opening of a second BOX unit. Still raising $NOSbF_6$ to three equivalents induces hyperchromic and hypsochromic effects on the main absorption band (552 nm) as well as the appearance of a higher energy band at 410 nm associated to the formation of the form **8**.

As consequence, based on previous results obtained under stimulation by acid (*vide supra*), we can assume that an electrochemical stimulation leads to observe the conversion of the different systems from forms **1** to **8** in a stepwise manner. Nevertheless, it does not allow to conclude about a possible regioselective addressability of the three BOX units in the case of unsymmetrical ones. For this reason, we have carried out the titration of **7a** (Figures S9 and S10) and 7b by $NOSbF_6$ by NMR (Figs. S14 and S15). As expected, the addition of $NOSbF_6$ in **7b** induces similar modification of the ^{19}F NMR spectrum as observed under the stimulation by acid. Eight different forms are detected and quantified by the integration of their corresponding signals (Fig. S15).

As already reported on other multi-BOX systems,[39] subtle differences are noticed between both kinds of stimulations. First, the successive BOX openings by chemical oxidation did not lead to its precipitation in ACN as previously observed with acid. Such a difference has been explained by the variation of the counterion from chloride to hexafluoro antimonate, a weakly coordinating anion leading to more lipophilic salt [56]. Second, the stimulation by an oxidizing agent appears as efficient as by an acid as demonstrated by the narrowed coexistence region between the **CCC** (form **1**), **OCC** (forms **2–4**), **OOC** (forms **5–7**) and **OOO** (form **8**)

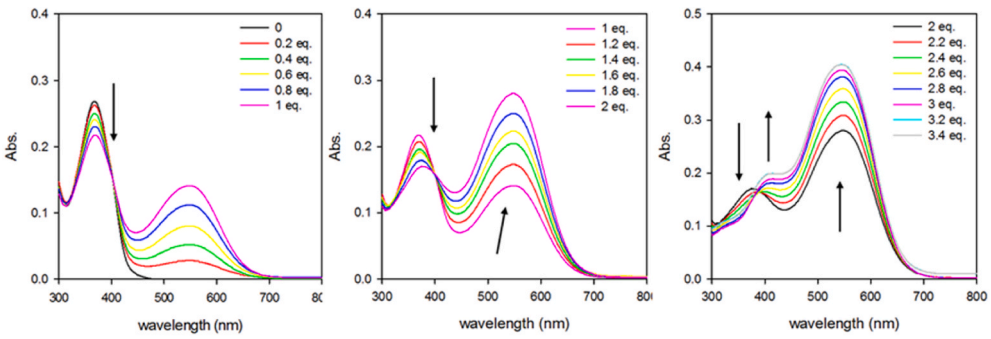

Fig. 7. Variation of the UV–Visible spectrum of **7b** (9 10^{-6}M) in ACN upon the addition of $NOSbF_6$ aliquots.

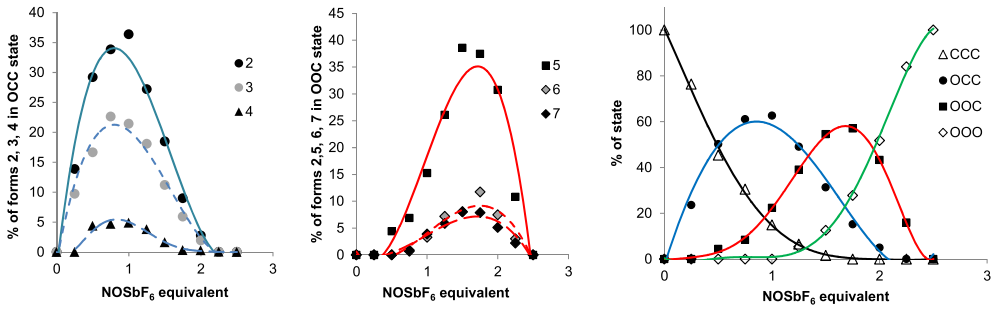

Fig. 8. Quantification of the forms in OCC and OOC states and of the 4 different states of compound **7b** (1 mM) in ACN upon addition of $NOSbF_6$ aliquots.

states (Fig. 8). Involving different processes, the modification of the nature of the stimulation presents surprisingly a moderate impact on the repartition of the different forms in **OCC** and **OOC** (Fig. 8**)**. As example, only a slight variation in the average composition of the **OCC** state is observed. The oxidation leads to 58; 37 and 5%, whereas acid provides 61; 33 and 6% of forms **2**, **3** and **4** respectively.

Theoretical calculation provides clues for the behavior of the different forms. First, the localization of the first oxidation process on the central π-conjugated core whatever the status of the different BOX units is well corroborated. The HOMO obtained by DFT calculation on **7c** under its different forms is mainly localized on the triarylamine in all cases (Fig. S1). More important, the switching of the system from forms **1** to **8** by the successive BOX openings in a stepwise manner is also well reproduced. In fact, the first oxidation potential of the system is strongly impacted by the number of open BOX units and also by the nature of their linker. As reported in Table S1, the calculated oxidation potentials for the 3 most preponderant forms are 0.23, 0.48 and 0.73V for forms **1**, **2**, and **5** respectively.

Up to now, the transformation of the system through an electromediated process has been explained through a multistep mechanism implying first the delocalization of the radical cation generated on the central π-conjugated system to the close vicinity of a BOX unit, second the C–O bond homolytic cleavage, and finally the abstraction of an hydrogen atom to the surrounding media [37,54,57]. Within this context, the Gibbs free energies for the opening of the radical cations were evaluated, showing that from its form **1**, the radical cation of **7c** preferentially leads to the form **2**, then the form **3** and the form **4**. Next, from the **OCC** state, the preferred pathways lead to forms **5**, **6**, and then **7**. The ordering of these Gibbs free energies has been rationalized in terms of geometrical considerations and in particular, the torsion angles between the aminium radical and the BOX systems. So, for the phenyl linker, there is a single angle with a departure from planarity and this angle is small ($\theta_C = 8°$) whereas for the phenylthienyl linker, the planarity is reduced ($\theta_B = 31°$ and $\theta_E = 0°$) and even more for the biphenyl linker ($\theta_A = 39°$ and $\theta_D = 14°$).

3. Conclusion

In our quest to elaborate more performant multi-chromophoric systems based on BOX unit, we have prepared and studied 4 symmetrical and 3 unsymmetrical systems involving three identical BOX units connected to each other by a central triarylamine core. As expected, all the systems have demonstrated some multimodal switching abilities allowing to use indifferently acid or electrochemical stimulation to address the three BOX units and consequentially to switch between the 4 different states from full closed state (**CCC**) to full open one (**OOO**). More important, we have demonstrated that the opening of the three BOX units occurs in a stepwise manner. As consequence, it was possible to generate on demand and in large excess the two intermediates **OCC** and **OOC** states. Resulting from two different processes (direct protonation or electromediated pathways), we have proved that the stepwise conversion of the system lays on strong interaction though bonds between the different units. In fact, the generation of an indoleninium moiety acting as a strong electron withdrawing group with the BOX opening induces a strong modification of the electronic properties of the central π-conjugated core.

Based on the same approach and using the steric hindrance to modulate the interaction of the different BOX units, we have explored the possibility to reach some regioselective addressability in place of a classical statistical opening. In this context, unsymmetrical systems bearing three identical BOX units connected to a central nitrogen atom by three different π-linkers (Ph, ThPh and PhPh) have demonstrated impressive behavior. If each one of their **OCC** and **OOC** states can theoretically exist under 3 different forms, the electrochemical and acid stimulations conduct to observe the predominant formation of one of those. Beside their easy synthesis and their multimodal switching ability, this possibility to cheat the statistical addressability by using simply a dissymmetric π-conjugated system is one more asset leading to consider the BOX unit as a switchable unit of choice for the elaboration of multi-switch systems.

CRediT authorship contribution statement

Youssef Aidibi: synthesis and characterization of the different tri-BOX derivatives, Data curation, Investigation. **Pierre Beaujean:** quantum chemistry calculations, quantum chemistry calculations, Validation, Data curation, Writing – review & editing. **Jean Quertinmont:** quantum chemistry calculations, quantum chemistry calculations, Methodology, Validation, Data curation. **Julien Stiennon:** quantum chemistry, Investigation. **Maxime Hodée:** quantum chemistry, Investigation. **Philippe Leriche:** Conceptualization, Project administration, Funding acquisition, Writing – review & editing. **Jérôme Berthet:** NMR, Investigation. **Stéphanie Delbaere:** NMR, Investigation, Conceptualization, Project administration, Funding acquisition, Writing – review & editing. **Benoît Champagne:** quantum chemistry calculations, Methodology, Validation, Data curation, Conceptualization, Project administration, Funding acquisition, Writing – review & editing. **Lionel Sanguinet:** Conceptualization, Project administration, Funding acquisition, Writing – review & editing.

Declaration of competing interest

The authors declare that they have no known competing financial interests or personal relationships that could have appeared to influence the work reported in this paper.

Acknowledgements

Y.A. thanks the University of Angers for granting. All authors thank the CARMA and ASTRAL platforms of the Structure Fédérative de Recherche MATRIX. This work, carried out within the MORIARTY project, has benefited from financial support from Wallonie-Bruxelles International (WBI), from the Fund for Scientific Research (F.R.S.-FNRS), from the French Ministry of Foreign and European Affairs, and

from the Ministry of Higher Education and Research in the frame of the Hubert Curien partnerships. The calculations were performed on the computers of the Consortium des Équipements de Calcul Intensif, including those of the Technological Platform of High-Performance Computing, for which we gratefully acknowledge the financial support of the FNRS-FRFC, of the Walloon Region, and of the University of Namur (Conventions 2.5020.11, GEQ U.G006.15, 1610468, and RW/GEQ2016).

Appendix B. Supplementary data

Supplementary data to this article can be found online at https://doi.org/10.1016/j.dyepig.2022.110270.

References

[1] Feringa BL. Molecular switches. Wiley-VCH Verlag GmbH; 2001i–xxii.
[2] Sachdeva T, Gupta S, Milton MD. Smart organic materials with acidochromic properties. Curr Org Chem 2020;24(17):1976–98.
[3] Nakatani K, Piard J, Yu P, Métivier R. Introduction: organic photochromic molecules. Photochromic Materials 2016:1–45.
[4] Minkin VI. Photo-, thermo-, solvato-, and electrochromic spiroheterocyclic compounds. Chem Rev 2004;104(5):2751–76.
[5] Seeboth A, Lotzsch D, Ruhmann R, Muehling O. Thermochromic polymers-function by design. Chem Rev 2014;114(5):3037–68.
[6] Di BH, Chen YL. Recent progress in organic mechanoluminescent materials. Chin Chem Lett 2018;29(2):245–51.
[7] Fu ZY, Wang K, Zou B. Recent advances in organic pressure-responsive luminescent materials. Chin Chem Lett 2019;30(11):1883–94.
[8] Goulet-Hanssens A, Eisenreich F, Hecht S. Enlightening materials with photoswitches. Adv Mater 2020;32(20):1905966.
[9] Credi A, Silvi S, Venturi M. Molecular machines and motors: recent advances and perspectives. 2014. Cham, Switzerland: Springer International Publishing; 2014.
[10] Zhang JL, Zhong JQ, Lin JD, Hu WP, Wu K, Xu GQ, Wee ATS, Chen W. Towards single molecule switches. Chem Soc Rev 2015;44(10):2998–3022.
[11] Andréasson J, Pischel U. Molecules with a sense of logic: a progress report. Chem Soc Rev 2015;44(5):1053–69.
[12] Andréasson J, Pischel U. Smart molecules at work - mimicking advanced logic operations. Chem Soc Rev 2010;39(1):174–88.
[13] Andreasson J, Pischel U. Storage and processing of information using molecules: the all-photonic approach with simple and multi-photochromic switches. Isr J Chem 2013;53(5):236–46.
[14] Oms O, Hakouk K, Dessapt R, Deniard P, Jobic S, Dolbecq A, et al. Photo- and electrochromic properties of covalently connected symmetrical and unsymmetrical spiropyran-polyoxometalate dyads. Chem Commun 2012;48(99):12103–5.
[15] Browne WR, Pollard MM, de lange B, Meetsma A, Feringa BL. Reversible three-state switching of luminescence: a new twist to electro and photochromic behavior. J Am Chem Soc 2006;128(38):12412–3.
[16] Ivashenko O, Logtenberg H, Areephong J, Coleman AC, Wesenhagen PV, Geertsema EM, et al. Remarkable stability of High energy conformers in self-assembled monolayers of a bistable electro- and photoswitchable overcrowded alkene. J Phys Chem C 2011;115(46):22965–75.
[17] Perrier A, Maurel F, Jacquemin D. Single molecule multiphotochromism with diarylethenes. Acc Chem Res 2012;45(8):1173–82.
[18] Chen J-X, Wang J-Y, Zhang Q-C, Chen Z-N. Multiphotochromism in an asymmetric ruthenium complex with two different dithienylethenes. Inorg Chem 2017;56(21):13257–66.
[19] Shukla J, Singh VP, Mukhopadhyay P. Molecular and supramolecular multiredox systems. ChemistryOpen 2020;9(3):304–24.
[20] Szaloki G, Pozzo J-L. Synthesis of symmetrical and nonsymmetrical bisthienylcyclopentenes. Chem Eur J 2013;19(34):11124–32.
[21] Fukaminato T. Single-molecule fluorescence photoswitching: design and synthesis of photoswitchable fluorescent molecules. J Photoch Photobio C 2011;12(3):177–208.
[22] Bertarelli C, Bianco A, Castagna R, Pariani G. Photochromism into optics: opportunities to develop light-triggered optical elements. J Photoch Photobio C 2011;12(2):106–25.
[23] Tsujioka T, Irie M. Electrical functions of photochromic molecules. J Photoch Photobio C 2010;11(1):1–14.
[24] Irie M. Photochromism of diarylethene single molecules and single crystals. Photochem Photobiol Sci 2010;9(12):1535–42.
[25] Irie M. Photochromism of diarylethene molecules and crystals. P JPN Acad B-Phys. 2010;86(5):472–83.
[26] Yun C, You J, Kim J, Huh J, Kim E. Photochromic fluorescence switching from diarylethenes and its applications. J Photoch Photobio C 2009;10(3):111–29.
[27] Wigglesworth TJ, Myles AJ, Branda NR. High-content photochromic polymers based on dithienylethenes. Eur J Org Chem 2005;7:1233–8.
[28] Tian H, Yang SJ. Recent progresses on diarylethene based photochromic switches. Chem Soc Rev 2004;33(2):85–97.
[29] Matsuda K, Irie M. Diarylethene as a photo switching unit. J Photoch Photobio C 2004;5(2):169–82.
[30] Irie M, Uchida K. Synthesis and properties of photochromic diarylethenes with heterocyclic aryl groups. Bull Chem Soc Jpn 1998;71(5):985–96.
[31] Harvey EC, Feringa BL, Vos JG, Browne WR, Pryce MT. Transition metal functionalized photo- and redox-switchable diarylethene based molecular switches. Coord Chem Rev 2015;282:77–86.
[32] Jacquemin D, Perpete EA, Maurel F, Perrier A. TD-DFT simulations of the electronic properties of star-shaped photochromes. Phys Chem Chem Phys 2010;12(28):7994–8000.
[33] Zhao F, Grubert L, Hecht S, Bléger D. Orthogonal switching in four-state azobenzene mixed-dimers. Chem Commun 2017;53(23):3323–6.
[34] Galanti A, Santoro J, Mannancherry R, Duez Q, Diez-Cabanes V, Valášek M, et al. A new class of rigid multi(azobenzene) switches featuring electronic decoupling: unravelling the isomerization in individual photochromes. J Am Chem Soc 2019;141(23):9273–83.
[35] Jeong M, Park J, Kwon S. Molecular switches and motors powered by orthogonal stimuli. Eur J Org Chem. 2020 2020;(47):7254–83.
[36] Zaitseva EL, Prokhoda AL, Kurkovskaya LN, Shifrina RR, Kardash NS, Drapkina DA, Krongauz VA. Photochromy of organic substances. VI. Preparation of N-methacryloylhydroxyethyl derivatives of indoline spiropyrans. Khimiya Geterotsiklicheskikh Soedin 1973;(10):1362–9.
[37] Szalóki G, Sanguinet L. Properties and applications of indolinooxazolidines as photo-, electro-, and acidochromic units. In: Yokoyama Y, Nakatani K, editors. Photon-working switches. Tokyo: Springer Japan; 2017. p. 69–91.
[38] Szaloki G, Sanguinet L. Silica-mediated synthesis of indolinooxazolidine-based molecular switches. J Org Chem 2015;80(8):3949–56.
[39] Sertova N, Nunzi JM, Petkov I, Deligeorgiev T. Photochromism of styryl cyanine dyes in solution. J Photochem Photobiol, A 1998;112(2,3):187–90.
[40] Petkov I, Charra F, Nunzi JM, Deligeorgiev T. Photochemistry of 2-[(1,3,3-trimethylindoline-2(1H)-ylidene)propen-1-yl]-3,3-dimethylindolino[1,2-b]-oxazolidine in solution. J Photochem Photobiol, A 1999;128(1–3):93–6.
[41] Hadji R, Szaloki G, Aleveque O, Levillain E, Sanguinet L. The stepwise oxidation of indolino[2,1-b]oxazolidine derivatives. J Electroanal Chem 2015;749:1–9.
[42] Szaloki G, Aleveque O, Pozzo J-L, Hadji R, Levillain E, Sanguinet L. Indolinooxazolidine: a versatile switchable unit. J Phys Chem B 2015;119(1):307–15.
[43] Sanguinet L, Berthet J, Szalóki G, Alévêque O, Pozzo J-L, Delbaere S. 13 metastable states arising from a simple multifunctional unimolecular system. Dyes Pigments 2017;137:490–8.
[44] Szalóki G, Sevez G, Berthet J, Pozzo J-L, Delbaere S. A simple molecule-based octastate switch. J Am Chem Soc 2014;136(39):13510–3.
[45] Aidibi Y, Guerrin C, Alévêque O, Leriche P, Delbaere S, Sanguinet L. BT-2-BOX: an assembly toward multimodal and multilevel molecular system simple as a breeze. J Phys Chem C 2019;123(18):11823–32.
[46] Guerrin C, Aidibi Y, Sanguinet L, Leriche P, Aloise S, Orio M, Delbaere S. When light and acid play Tic-Tac-Toe with a nine-state molecular switch. J Am Chem Soc 2019;141(48):19151–60.
[47] Wang J, Liu K, Ma L, Zhan X. Triarylamine: versatile platform for organic, dye-sensitized, and perovskite solar cells. Chem Rev 2016;116(23):14675–725.
[48] Hayami M, Torikoshi S. Color-changing compounds. Japan: Matsushita Electric Industrial Co., Ltd.; 1976. p. 46.
[49] Pielak K, Tonnelé C, Sanguinet L, Cariati E, Righetto S, Muccioli L, Castet F, Champagne B. Dynamical behavior and second harmonic generation responses in acido-triggered molecular switches. J Phys Chem C 2018;122(45):26160–8.
[50] Hadj Mohamed S, Quertinmont J, Delbaere S, Sanguinet L, Champagne B. Assessing the structure of octastate molecular switches using 1H NMR density functional theory calculations. J Phys Chem C 2018;122(3):1800–8.
[51] Nelson RR, Adams RN. Anodic oxidation pathways of substituted triphenylamines. II. Quantitative studies of benzidine formation. J Am Chem Soc 1968;90(15):3925–30.
[52] Seo ET, Nelson RF, Fritsch JM, Marcoux LS, Leedy DW, Adams RN. Anodic oxidation pathways of aromatic amines. Electrochemical and electron paramagnetic resonance studies. J Am Chem Soc 1966;88(15):3498–503.
[53] Thelakkat M. Star-Shaped, dendrimeric and polymeric triarylamines as photoconductors and hole Transport materials for electro-optical applications. Macromol Mater Eng 2002;287(7):442–61.
[54] Quertinmont J, Beaujean P, Stiennon J, Aidibi Y, Leriche P, Rodriguez V, Sanguinet L, Champagne B. Combining benzazolo-oxazolidine Twins toward multi-state nonlinear optical switches. J Phys Chem B 2021;125(15):3918–31.
[55] Kochi JK. Inner-sphere electron transfer in organic chemistry. Relevance to electrophilic aromatic nitration. Acc Chem Res 1992;25(1):39–47.
[56] Longo LS, Smith EF, Licence P. Study of the stability of 1-Alkyl-3-methylimidazolium hexafluoroantimonate(V) based ionic liquids using X-ray photoelectron spectroscopy. ACS Sustainable Chem Eng 2016;4(11):5953–62.
[57] Bondu F, Hadji R, Szaloki G, Aleveque O, Sanguinet L, Pozzo J-L, Cavagnat D, Buffeteau T, Rodriguez V. Huge electro-/photo-/acidoinduced second-order nonlinear contrasts from multiaddressable indolinooxazolodine. J Phys Chem B 2015;119(22):6758–65.